Original Article

OPEN

Extrauterine growth restriction on pulmonary vascular endothelial dysfunction in adult male rats: the role of epigenetic mechanisms

Liyan Zhang[a], Lili Tang[a], Jiakai Wei[a], Linjiang Lao[a], Weizhong Gu[b], Qiongyao Hu[a], Ying Lv[a], Linchen Fu[a], and Lizhong Du[a]

Objective: Early postnatal life is considered as a critical time window for the determination of long-term metabolic states and organ functions. Extrauterine growth restriction (EUGR) causes the development of adult-onset chronic diseases, including pulmonary hypertension. However, the effects of nutritional disadvantages during the early postnatal period on pulmonary vascular consequences in later life are not fully understood. Our study was designed to test whether epigenetics dysregulation mediates the cellular memory of this early postnatal event.

Methods and results: To test this hypothesis, we isolated pulmonary vascular endothelial cells by magnetic-activated cell sorting from EUGR and control rats. A postnatal insult, nutritional restriction-induced EUGR caused development of an increased pulmonary artery pressure at 9 weeks of age in male Sprague–Dawley rats. Methyl-DNA immune precipitation chip, genome-scale mapping studies to search for differentially methylated loci between control and EUGR rats, revealed significant difference in cytosine methylation between EUGR and control rats. EUGR changes the cytosine methylation at approximately 500 loci in male rats at 9 weeks of age, preceding the development of pulmonary hypertension and these represent the candidate loci for mediating the pathogenesis of pulmonary vascular disease that occurs later in life. Gene ontology analysis on differentially methylated genes showed that hypermethylated genes in EUGR are vascular development-associated genes and hypomethylated genes in EUGR are late-differentiation-associated and signal transduction genes. We validated candidate dysregulated loci with the quantitative assays of cytosine methylation and gene expressions.

Conclusion: These results demonstrate that epigenetics dysregulation is a strong mechanism for propagating the cellular memory of early postnatal events, causing changes in the expression of genes and long-term susceptibility to pulmonary hypertension, and further providing a new insight into the prevention and treatment of EUGR-related pulmonary hypertension.

Keywords: endothelial cell, epigenetics, extrauterine growth restriction, pulmonary hypertension

Abbreviations: ChIP, chromatin immunoprecipitation; DOHaD, developmental origins of health and disease; eNOS, endothelial nitric oxide synthase; EUGR, extrauterine growth restriction; GEO, gene expression omnibus; GO, gene ontology; IGF-1, insulin-like growth factor-1; IUGR, intrauterine growth restriction; MACS, magnetic-activated cell sorting; MeDIP-chip, methyl-DNA immune precipitation chip; PH, pulmonary hypertension; PPARγ, peroxisome proliferator-activated receptor gamma; PPHN, persistent pulmonary hypertension of the newborn; PVECs, pulmonary vascular endothelial cells; ROI, region of interest; TSS, transcription start site

INTRODUCTION

Many epidemiologic and experimental studies support the developmental origins of health and disease (DOHaD) hypothesis [1]. Early postnatal life is considered as a critical time window for the determination of long-term metabolic states and organ functions. Intrauterine growth restriction (IUGR) or extrauterine growth restriction (EUGR) resulting from undernutrition is associated with an increased risk of neonatal lung disease as well as adult-onset diseases, including hypertension and other cardiovascular diseases [2–6]. Persistent pulmonary hypertension of the newborn (PPHN) is a clinical syndrome of hypoxemic respiratory failure characterized by abnormal pulmonary vascular tone, reactivity and structure [7]. IUGR, mainly uteroplacental insufficiency, is one of the important causes of increased pulmonary vascular reactivity during adulthood [8]. In humans of low birth weight, endothelium-dependent vasodilation is generally impaired [9]. Recent studies have shown that endothelial dysfunction is associated with the rate of growth in the first month of life in

Journal of Hypertension 2014, 32:2188–2198

[a]Department of Neonatology and [b]Department of Pathology, The Children's Hospital, Zhejiang University School of Medicine, Hangzhou, P.R. China

Correspondence to Lizhong Du, Professor, The Children's Hospital, Zhejiang University School of Medicine, Hangzhou 310003, P.R. China. Tel: +86 571 87068247; fax: +86 571 87033296; e-mail: dulizhong@zju.edu.cn

Received 5 February 2014 **Revised** 11 June 2014 **Accepted** 11 June 2014

DOI:10.1097/HJH.0000000000000309

infants [10], and changes in DNA methylation are associated with different weight loss response patterns in obese or overweight adolescents [11].

Although the mechanisms of nutritional programming in the development of pulmonary hypertension remain unclear, epigenetics seems to play a key role, potentially explaining how environmental factors can influence later development by resetting the structure and function of the pulmonary vasculature. The maternal environment during gestation can alter the epigenome of the offspring and thus give rise to different phenotypes [12,13]. IUGR impairs alveolarization in conjunction with the altered expression of peroxisome proliferator-activated receptor gamma (PPARγ), elastin and insulin-like growth factor-1 (IGF-1) through epigenetic modifications in rat [14,15], and lungs are the organs where epigenetic modulators are the most affected in rats in a IUGR model [16]. Abnormal pulmonary vascular responsiveness in the offspring of pregnant mice fed with a restrictive diet was observed in both normoxic and hypoxic conditions [17].

Our recent study demonstrated an upregulation of endothelial nitric oxide synthase (eNOS) expression that associated with epigenetic modifications in *eNOS* gene in PVECs derived from a neonatal rodent PPHN model [18], and epigenetics is closely associated with the development of hypoxic pulmonary hypertension following IUGR [19]. Recent evidence suggests that the development and progression of vascular disease, including atherosclerosis, coronary heart disease and hypertension, are associated with a reduced nitric oxide production [20].

On the basis of the evidence that epigenetics plays an important role in the developmental origins of adult disease, we hypothesized that a postnatal insult of EUGR could cause epigenetic modification of the genes that are related to lung development and pulmonary vascular tone regulation in later life. To test this hypothesis, a EUGR rat model was induced by litter-size-adjusted postnatal nutritional restriction [21]. We investigated the methylation status of global DNA to search for differentially methylated loci by methyl-DNA immune precipitation chip (MeDIP-chip), and the cytosine methylation and histone modification of the *eNOS*, *IGF-1* and *PPARγ* genes.

MATERIALS AND METHODS

Extrauterine growth restriction rat model

This study was carried out in strict accordance with the recommendations in the Guide for the Care and Use of Laboratory Animals of the National Institutes of Health. All procedures and protocols were approved by the Animal Care and Use Committee of Zhejiang University. All surgery was performed under anesthesia, and all efforts were made to minimize suffering. Pregnant Sprague–Dawley rats obtained from Zhejiang University Laboratory Animal Center and were kept in the same room with a constant temperature maintained at $22 \pm 3^{\circ}$C, and allowed to drink water freely. Within 12 h of birth, pups were weighed and randomly assigned to either a control litter, consisting of 10 pups, or a large litter consisting of 20 pups, both with a 1 : 1 male-to-female ratio. This model has been demonstrated to lead to equal growth restriction in each of the pups of the large litter [22]. Pups' weights were recorded daily until weaning. On day 21, those pups in large litters whose weight was less than the 10th percentile of the control litter were defined as EUGR [23]. On day 21, the pups were weaned and male rats were housed two per cage until 9 weeks of age. Offspring were weighed twice a week during the first month of postnatal life and once a week thereafter until 9 weeks of age. To avoid the variability of the results related to the hormonal cycle in female rats, only male offspring were studied.

Assessment of pulmonary arterial pressure

Nine-week-old male rats were anesthetized with chloral hydrate (100–400 mg/kg) which was administered subcutaneously and placed on a thermo-regulated surgical table. A PE50 catheter was inserted into the right jugular vein. With the angle directed anteriorly, the catheter was inserted 25 mm proximally, which placed the catheter in the right atrium. The catheter was rotated 90° anticlockwise and inserted 10 mm further, which placed the catheter in the right ventricle (RV), and when advanced an additional 10 mm, in the pulmonary artery. Placement at each stage was confirmed by respective pressure contours. Hemodynamic values were automatically calculated by a physiological data acquisition system (Acqknowledge4.MP150; Biopac System Inc., Goleta, California, USA). Following exsanguination, the lungs were distended by infusion of phosphate buffer saline (PBS) into the trachea, quickly frozen in liquid nitrogen or infused with 10% formalin and fixed over 8 h. For Fulton's index of right ventricular hypertrophy, the ratio of the right ventricle to left ventricle weight and septal weight (RV/LV + S) was calculated [24].

Immunohistochemistry and physical measurements

Right lung tissues of different ages were isolated, frozen in liquid nitrogen and stored at −80°C. Left lung tissues of different ages were isolated and perfused with ice-cold 10% formalin at a pressure of 25 cm H_2O and fixed for 24 h at 4°C. The lung tissues were imbedded in paraffin, sectioned at 4–5 μm, and processed for light microscopic immunohistochemistry as the previously described [18,25]. Samples were incubated with a primary antibody against smooth-muscle-specific alpha-actin (α-SMA, clone:1A4; Dako, Denmark) overnight, followed by secondary goat antibody (HRP polymer) for 30 min at 37°C. At least eight slides from each lung were taken and then analyzed.

The percentage of pulmonary arterial medial thickness occupied by smooth muscle was determined according to our previous study [18]. Small pulmonary arteries of 50–150 μm in diameter were investigated via a systematic sampling method to evaluate random, nonoverlapping calibrated fields for each variable. The terminal bronchioles were used as an independent landmark for selecting small pulmonary arteries. We used Image Pro Plus software (Media Cybernetics, Bethesda, Maryland, USA) to make the measurements. Tissue slides were analyzed by a technician who was without knowledge of the group from which the tissue was taken.

Isolation of pulmonary vascular endothelial cells

Pulmonary vascular endothelial cells (PVECs) from the above animals were isolated by magnetic-activated cell sorting (MACS) as described in our previous study [18]. Fresh rat lungs were sliced and then incubated with collagenase A. The suspensions were filtered, centrifuged and washed three times in PBS containing 0.5% bovine serum albumin (BSA) and 2 mmol/l EDTA. The final pellets were resuspended in 100 μl of PBS with 0.5% BSA and 2 mmol/l EDTA per 10^7 total cells, and then incubated with PECAM-1 (555027, BD PharMingen, San Diego, California, USA) for 15 min at 4°C. After washing, anti-PE MicroBeads (130-048-801, Miltenyi Biotec, Bergisch Gladbach, Germany) were added to the cell suspension for 15 min at 4°C. The PVEC positively labeled with the magnetic microbeads that linked to PECAM-1 antibody were selected with the separation unit and kept at −80°C until use. The proportion of positive PVEC after MACS was about 92%, there were no statistically significant difference between groups.

Quantitative RT-PCR

Total RNA was isolated from PVECs according to the RNeasy protocol (Axygen, Central Avenue Union City, California, USA) RNA was reverse transcribed using a reverse transcriptase kit (TAKARA; TaKara Bio, Dalian, China) according to the manufacturer protocols. Real-time quantitative PCR was performed by the ABI Prism 7500 Instrument following the TAKARA protocol. β-Actin was used as an internal control. Primers are shown in supplementary material Table S1, http://links.lww.com/HJH/A378.

Chromatin immunoprecipitation

Chromatin immunoprecipitation (ChIP) assay was performed as described in a previous study [18]. After the isolated PVEC were fixed and cross-linked, the cell pellets were suspended in cell lysis buffer and centrifuged, and the supernatants were discarded. The pellets were resuspended in SDS lysis buffer, sonicated, centrifuged and aliquots of soluble chromatin were collected. Aliquots of the supernatants were retained for representing the input chromatin. Aliquots were incubated overnight at 4°C with one of the following antibodies: 5 μl H3K9ace (Millipore 07-352; Billerica, Massachusetts, USA), 5 μl H3K4met3 (Millipore 17-614), 5 μl H3K9met3 (Millipore 17-625) and 5 μl H3K27met3 (Millipore 07-449). The immune complexes were precipitated with Protein A beads and then eluted. The input, unbound and bound fractions were incubated with 5 mol/l NaCl to reverse crosslink. The DNA fragments were purified using the Qiaquick PCR Purification kit (Qiagen, Hilden, Germany). The DNA fragments containing genes site-specific sequences were quantified by real-time PCR. Relative quantification of PCR products were based on the value differences between the bound and input using the $^{\Delta\Delta}$Ct method. The PCR primers for the gene are shown in supplementary material Table S2http://links.lww.com/HJH/A378.

DNA methylation profiling by methyl-DNA immune precipitation chip

The methylation status of global DNA of individual samples was determined by MeDIP-chip using the MeDIP-chip kit, according to the Nimblegen MeDIP-chip protocol (Capital-Bio, Beijing, China). Genomic DNA was extracted from the individual tissue samples and digested into 200–1000 bp of random fragments as starting material and 1 μg antibody against 5-methylcytidine (ab10805, Abcam, Cambridge, Massachusetts, USA). The labeled DNA samples were combined and hybridized to Rat 3 × 720K Multiplex CpG Island Plus-Ref-Seq Promoter Array (BD PharMingen). Each array covers 15 790 annotated CpG islands as well as 15 287 promoters (design region is from about −3880 bp to +970 bp of the TSSs) of the well characterized RefSeq genes derived from the UCSC RefFlat files. After washing, the arrays were scanned using a MS200 scanner (BD PharMingen).

Microarray data has been uploaded to the gene expression omnibus (GEO) database and can be accessed via the following link: http://www.ncbi.nlm.nih.gov/geo/query/acc.cgi?acc=GSE48648.

Methyl-DNA immune precipitation chip data analysis and bioinformatics

Data were extracted and exported to excel using NimbleScan. Raw excel data files obtained from tiling array experiments were analyzed using NimbleScan2.3 software. The ratios of Cy5 to Cy3 signals were calculated for all high-quality hybridization dots, normalized and transformed to log2 ratio. From the normalized log2-ratio data, a sliding-window (750 bp) peak-finding algorithm provided by NimbleScan v2.5 (Roche-NimbleGen) is applied to analysis the MeDIP-chip data. One-side Kolmogorov–Smirnov test was conducted to obtain P value (−Log10 P-value) of each probe. Peak score was generated by the interval analysis with a cutoff value of 2, maximum gap at 500 bp and a minimum run with at least two consecutive probes. The regions with peak scores were defined as methylated, and the level of methylation was a positive correlation with peak scores. If the methylation frequency of a region in EUGR was significantly higher than that in the control PVECs, we defined the region as a hypermethylation region. On the contrary, we defined it as a hypomethylation region. GFF files of $\log_2$ ratio, *P* value, peak score and array annotation data were exported to Signalmap 1.0 software for visual analysis and review. Data analysis was performed using Molecular Annotation system 3.0 (KANGCHEN Bio-tech., Shanghai, China). Gene Ontology and pathway analysis was performed using the DAVID bioinformatics tool (david.abcc.ncifcrf.gov/) [26] and ingenuity pathway analysis (http://www.ingenuity.com) under the default settings.

MeDIP-chip data analysis result are summarized in the online supplemental section from KANGCHEN Bio-tech.; http://links.lww.com/HJH/A378, http://links.lww.com/HJH/ A379, http://links.lww.com/HJH/A380, http://links.lww.com/HJH/A381, China (http://kcbiochip.bioon.com.cn/). The MA plots (The MA-plot is a plot of the distribution of red/green intensity ratio ('M') plotted by the average intensity ('A'). M and A are defined by the following equations.) and box plots were applied to assess the quality of raw data and effect of Normalization. [A MA-plot is a plot of the distribution of the red/green intensity ratio (*M*) plotted against the average intensity (*A*). *M* and *A* are defined by the following equations: $M = \log_2 R - \log_2 G$ and $A = (1/2) \times (\log_2 R + \log_2 G$, where *R* and *G*

represent the probe raw signal intensity for the MeDIP and Input channels, respectively.] A correlation matrix was used to describe the correlation among replicate experiments. Region of interest (ROI) analysis was done using mean $\log_2$ ratio across defined regions (probe number in −700 to +200 bp relative to the transcription start site). Clustering gene-expression data analysis was done using Cluster Manager (MeV v4.7.4) [27].

On the basis of their entire CpG contents across the genomic region, gene promoters have been recently classified into one of three categories: high CpG promoter (HCP that contains a 500 bp region with a GC content ≥0.55 and a CpG observed to expected ratio ≥0.6), low CpG promoter (LCP containing no 500 bp interval and with a CpG observed to expected ratio ≥0.4), and intermediate CpG content promoter (ICP with CpG density between HCP and ICP) using the dataset generated by Mikkelsen [28].

MassARRAY measurements of DNA methylation

The Sequenom Mass ARRAY platform (CapitalBio) was used for the quantitative analysis of methylation. Further experimental analysis of the contents of DNA methylation was determined, as described previously [29]. Primer sets and the target DNA region length and number of CpGs for the quantitative analysis of methylation are shown in the supplementary material Tables S3 and S4 http://links.lww.com/HJH/A378.

Statistical analysis

At least three biological replicates were performed in the experiments, unless stated otherwise. Data were expressed as mean ± SEM. The levels of methylation in the specific gene of individual samples were calculated, according to the percentage of methylation in all CpG sites of the target promoter regions. The difference in the levels of methylation between EUGR samples and control individuals was analyzed by one-way analysis of variance (ANOVA), and the difference in the levels of gene expression and tissue samples was analyzed by Student's *t*-test The potential correlation between gene expression and methylation levels was determined by Pearson correlation and linear regression analysis. A P value less than 0.05 was considered statistically significant.

RESULTS

Body weight and postnatal growth

On day 1, before the groups were assigned, there were no significant differences between EUGR and control rats for body weight ($P = 0.849$). From day 4 until the end of the experiment around 9 weeks, body weight was significantly

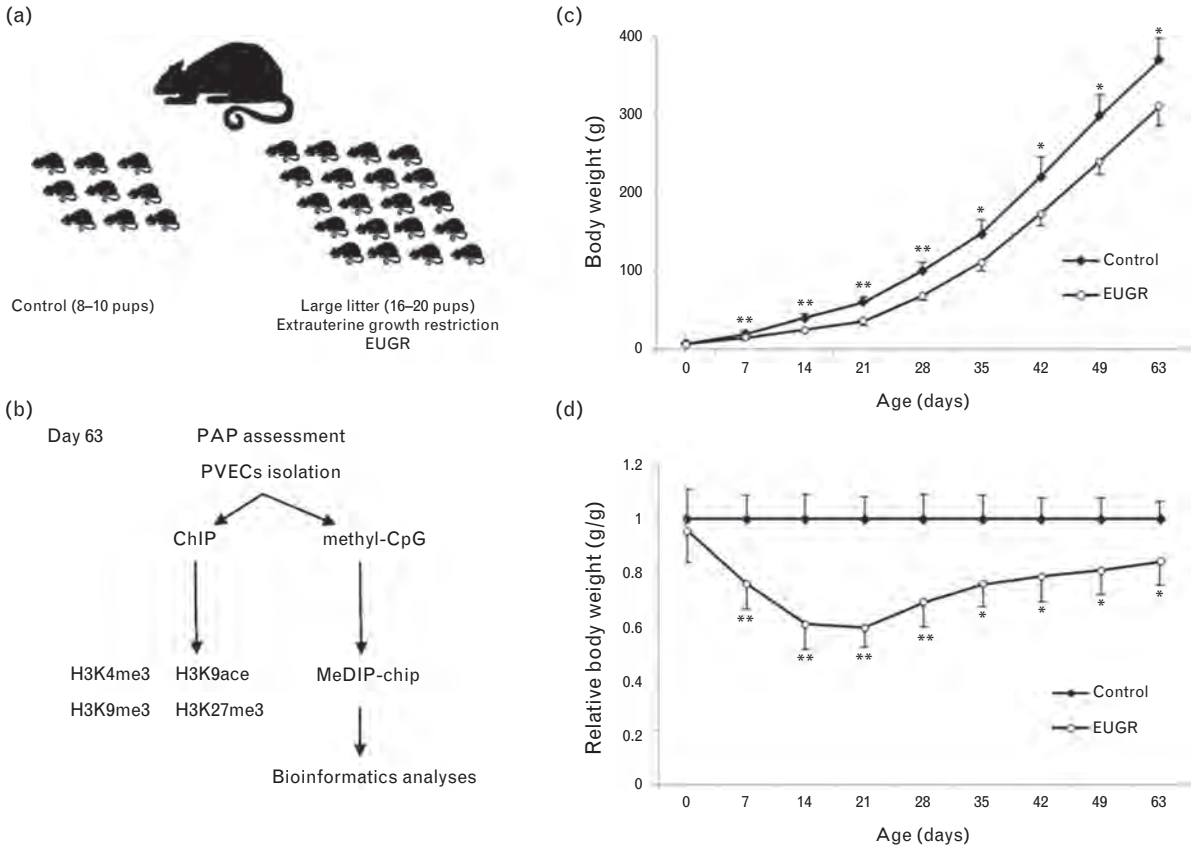

FIGURE 1 Body weight of EUGR male rats is persistently less than the control rats. (a) Overview of the litter size experiment. Sprague–Dawley rats were cross-fostered at day 1 and randomly assigned to EUGR or control litters. (b) Assessment of PAP and PVECs isolation were performed at day 63. (c) Body weight of EUGR (o) and Control (◆) rats did not differ at day 1. EUGR showed significantly less body weight at day 21 which was maintained till adulthood (day 63). (d) Body weight relative to the control mean at the same age. Values are means ± SD. $^{*}P < 0.05$; $^{**}P < 0.01$; $n \geq 20$ animals in each group. EUGR, extrauterine growth restriction; PAP, pulmonary arterial pressure; PVECs, pulmonary vascular endothelial cells.

less in EUGR animals than in controls ($P < 0.05$; see Fig. 1b). In EUGR rats, all relative body dimensions decreased during lactation, followed by a rapid but incomplete catch-up growth after weaning, when all animals had unlimited access to food. This pattern is shown in Fig. 1c for relative body weight.

Extrauterine growth restriction male rats developed increased pulmonary artery pressure at day 63

We next examined the right ventricular systolic pressure (RVSP) and the pulmonary artery pressure (PAP) at 63-day-old male rats. We found that EUGR rats developed increased RVSP and PAP compared with controls to some degrees. PAP was 19.23 ± 1.34 mmHg in control rats vs. 26.69 ± 2.51 mmHg in EUGR rats ($P < 0.05$; Fig. 2a). RVSP was 14.53 ± 2.34 mmHg in control rats vs. 19.69 ± 2.11 mmHg in EUGR rats ($P < 0.05$). And, right ventricle-to-left ventricle and septum (RV to LV + S) weight ratio was significantly higher in EUGR compared with control rats (Fig. 2b).

Pulmonary vascular histological changes

The percentage of medial thickness in the small pulmonary arteries of 50–150 μm diameter was analyzed. Note the significant medial thickness (Fig. 2d), and a prominent obstructive intimal thickening at the level of small arteries and arterioles was observed in EUGR group.

Extrauterine growth restriction reduces endothelial nitric oxide synthase expression in adult male rats

The eNOS expression level in the EUGR male rats was lower than that in the controls, and there was a statistically significant difference between the two groups ($P = 0.032$; Fig. 2g). Similar to the protein expression pattern, the eNOS

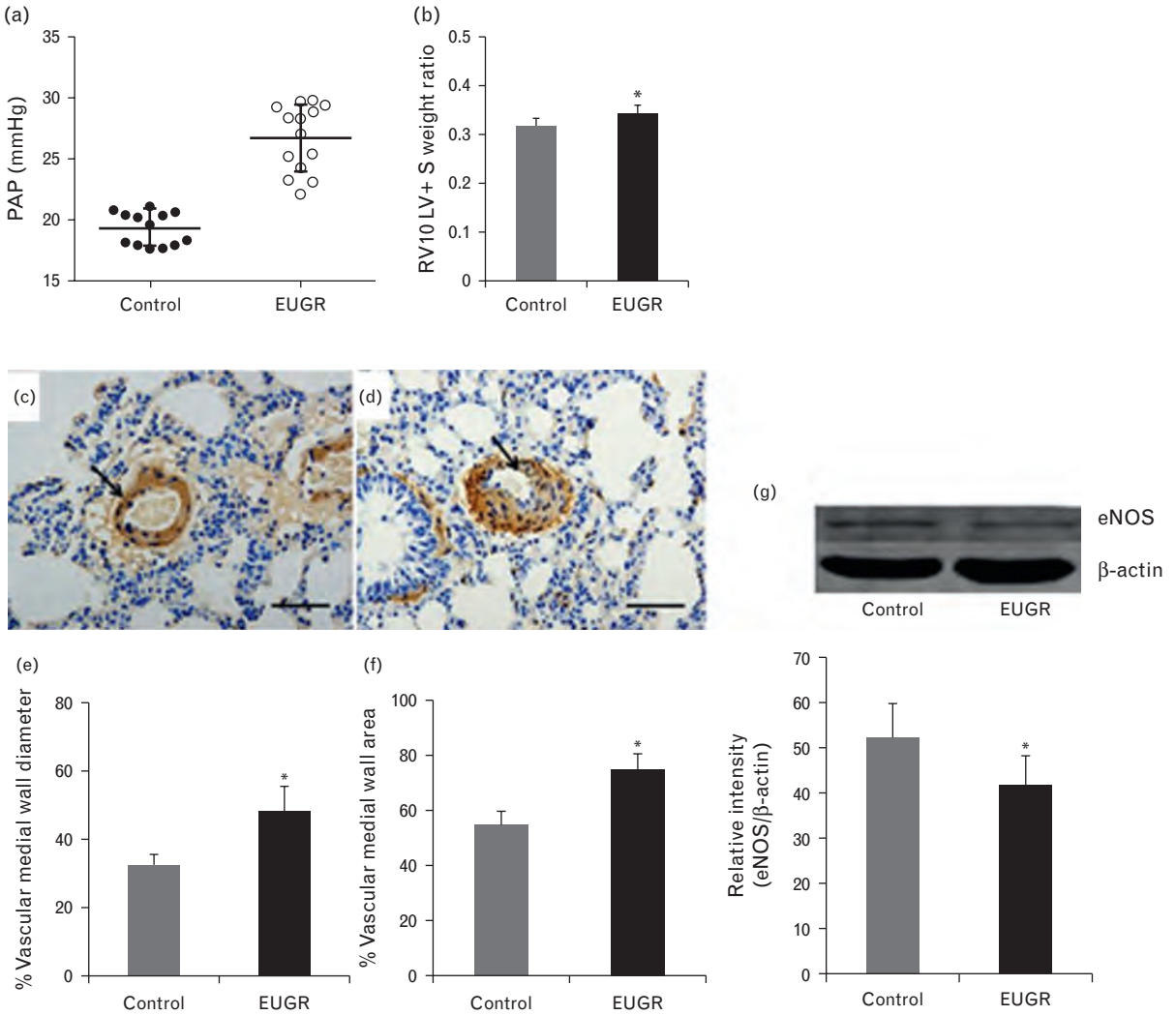

FIGURE 2 EUGR male rats developed increased pulmonary artery pressure at 9 weeks of age. Pulmonary artery pressure (PAP; a) and right ventricle-to-left ventricle and septum (RV to LV + S) weight ratio (b) in EUGR and control rats are shown at 9 weeks of age. Representative lung histological sections of controls (c) and EUGR (d) are shown, demonstrating hypertrophy of the arterial medial wall induced by EUGR. Note significant medial thickness (d), and the prominent obstructive intimal thickening at the level of small arteries and arterioles was observed in EUGR group (200×). The bar graph represents the %vascular medial wall diameter (e) and percentage vascular medial wall area (f) of the small pulmonary arteries. (g) eNOS protein expression in PVEC. Western blots for eNOS utilize beta-actin as an internal control. Note that eNOS protein level in EUGR was significantly lower than that in the control ($n = 5$–6; $^*P < 0.05$). eNOS, endothelial nitric oxide synthase; EUGR, extrauterine growth restriction; PVECs, pulmonary vascular endothelial cells.

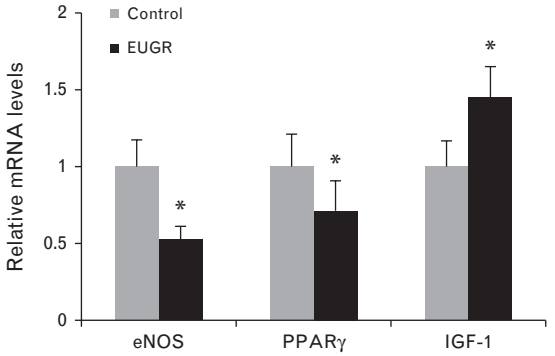

FIGURE 3 Quantitative RT-PCR shows the change of *eNOS*, *PPARγ* and *IGF-1* genes in mRNA expression. Average $\log_2$ ratio (± SEM) of EUGR expression data relative to controls was calculated for each gene. $n = 6$–8, $^*P < 0.05$. eNOS, endothelial nitric oxide synthase; IGF-1, insulin-like growth factor-1; PPARγ, peroxisome proliferator-activated receptor gamma.

mRNA expression showed a similar trend (Fig. 3). These results indicate that the decreased eNOS level of EUGR rats might be responsible for the increased PAP and pulmonary vascular remodeling changes.

Identification of differential methylation regions in the whole genome of pulmonary vascular endothelial cells between extrauterine growth restriction and control rats

We performed a whole-genome cytosine methylation assay on PVECs isolated at 9-week-old male rats and confirmed the overall data quality for each sample as previously described [30]. The methylation status in the promoter is associated with the regulation of gene expression. ROI analysis was done using mean $\log_2$ ratio across defined regions (probe number in −700 to +200 bp relative to the transcription start site), this clustering approach showed significant differences in cytosine methylation between EUGR and controls (Fig. 4a). The EUGR and control group comparisons revealed consistently and distinctively methylated loci, with approximately 500 changes in methylation loci enriched for highly significant group differences.

Profile the promoter methylation pattern (see Fig. S1, http://links.lww.com/HJH/A378). Hypomethylated and hypermethylated regions were identified in the EUGR PVECs. Among these regions, 488 hypomethylated and 216 hypermethylated regions were CpG islands (Fig. S1b, http://links.lww.com/HJH/A378). Some hypomethylated (244) and hypermethylated (38) regions were mapped to both the promoters of known genes and CpG islands (Fig. S1c, http://links.lww.com/HJH/A378). We found that in the pool of hypomethylated genes, 53.6% of them belong to the HCP cluster, which is much lower than the genome average (67%) (Fig. S1d, http://links.lww.com/HJH/A378). In contrast, in the pool of hypermethylated genes, over 46% of genes are considered HCP promoters (Fig. S1d, http://links.lww.com/HJH/A378). Notably, 50% of hypomethylated and 17.60% of hypermethylated regions were mapped to the promoter regions of known genes (Fig. S1e,

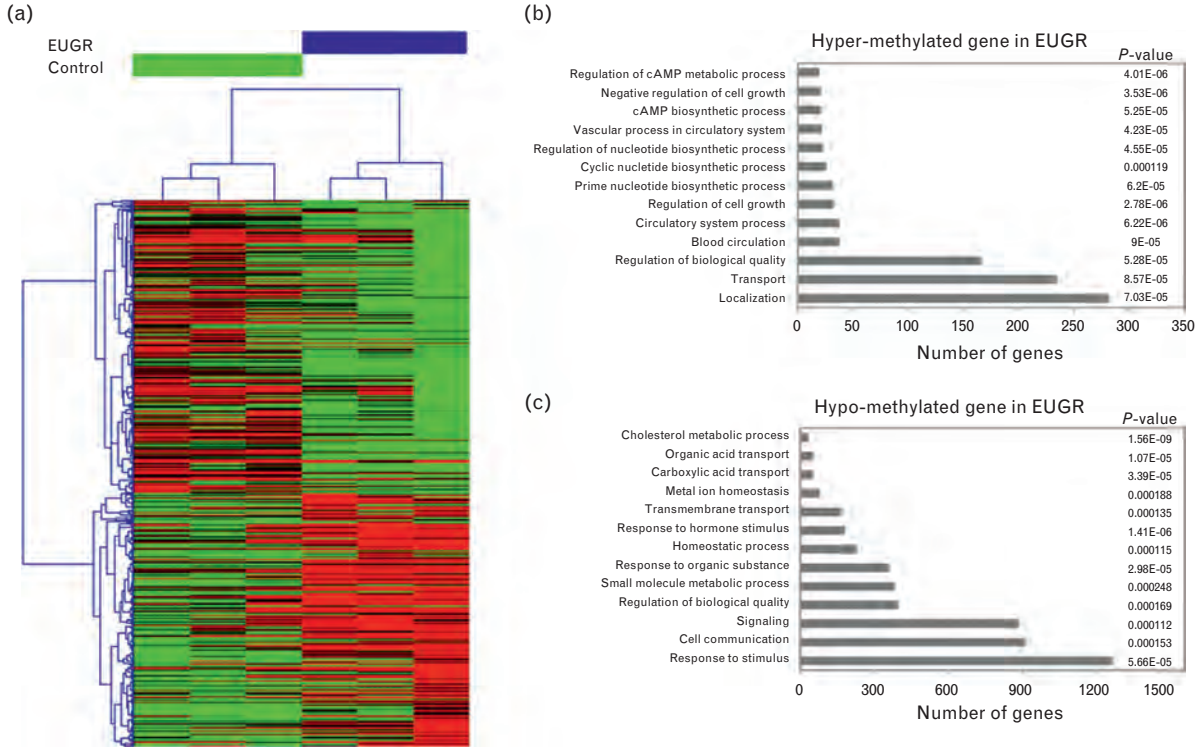

FIGURE 4 Significant differences in cytosine methylation between EUGR and control rats. Region of interest (ROI) analysis was done using mean $\log_2$ ratio across defined regions (probe number in −700 to +200 bp relative to the TSS), calculated using multiexperiment viewer (MeV v4.7.4). Data come from MeDIP-chip. We isolated PVECs by MACS from controls ($n = 3$) and EUGR ($n = 3$). (a) Heat map of the approximately 500 loci showed that distinguish EUGR from control rats. Each row in this heat map corresponds to data from a single locus, whereas columns correspond to individual samples. EUGR and controls show similar numbers of loci becoming relatively hypermethylated and hypomethylated (red to green, respectively). Gene ontology classifications for hypermethylated (b) and hypomethylated (c) genes. The GO term is on the *y* axis, number of gene is on the *x* axis, and the *P*-value indicating significance of enrichment is on the right side. EUGR, extrauterine growth restriction; GO, gene ontology; MACS, magnetic-activated cell sorting; PVECs, pulmonary vascular endothelial cells.

http://links.lww.com/HJH/A378). Thus, there are many novel differential methylation regions (DMRs) in the promoters, intergenic, intragenic of known genes and unannotated genomic regions in EUGR PVECs. The methylation status in the promoter is associated with the regulation of gene expression. We further analyzed the DMRs mapped to the gene promoters in EUGR, and the 209 hypermethylated and 468 hypomethylated promoters identified by MeDIP-chip were distributed in different loci and chromosomes (Fig. S1f, http://links.lww.com/HJH/A378). Although the promoter-hypermethylated genes were present predominately in the 1, 5, 12, 14 and 19 chromosomes, small numbers of the promoter-hypermethylated genes also occurred in other chromosomes. Interestingly, the promoter-hypomethylated genes were mainly distributed in the 1, 3, 7, 10, 12 and 18 chromosomes.

Gene ontology analysis of hypermethylated vs. hypomethylated promoters in pulmonary vascular endothelial cells

In order to more fully understand any biological and cell functions subject to coordinated regulation in the endothelial cells between our animal cohorts, we performed gene ontology analyses on differentially methylated genes. The most highly represented categories and their *P*-values for the dysregulated genes of methylation are shown in Fig. 3b and c. Hypermethylated genes in EUGR were enriched for a number of categories of genes involved in location ($P < 7 \times 10^{-5}$), blood circulation ($P < 9 \times 10^{-5}$), circulatory system process ($P < 6 \times 10^{-6}$) and vascular process in circulatory system ($P < 4 \times 10^{-5}$). This suggests that genes that exhibit DNA hypermethylation are vascular-development-associated genes. Hypomethylated genes were enriched for gene ontology annotations such as response to stimulus ($P < 5 \times 10^{-5}$), signaling ($P < 1 \times 10^{-4}$), response to hormone stimulus ($P < 1.4 \times 10^{-6}$) and cholesterol metabolic process ($P < 1.5 \times 10^{-9}$). This result suggests that genes that exhibit DNA hypomethylation are late-differentiation-associated and signal transduction genes.

We also performed pathway analysis of these differential promoter-methylated genes using the DAVID bioinformatics tools [26]. For pathway analysis, see Fig. S2 and for data result see online supplemental section, http://links.lww.com/HJH/A378, http://links.lww.com/HJH/A379, http://links.lww.com/HJH/A380, http://links.lww.com/HJH/A381. Some of the genes, such as events in the calcium, Notch, vascular endothelial growth factor (VEGF), TGF-beta, ErbB, Insulin, Wnt and mitogen-activated protein kinase (MAPK) signal pathways, were also involved in regulating the development of pulmonary hypertension. In addition, several of the promoter-hypermethylated genes were associated with the development of pulmonary hypertension and these include Fgfr2, Rhoc and Notch1. Apparently, the research strategies and the resulting data are valuable for the evaluation of the significance of DMRs in EUGR PVECs. EUGR changes cytosine methylation at approximately 500 loci in male rats at 9 weeks of age, preceding the development of pulmonary hypertension and these represent the candidate loci for mediating the pathogenesis of pulmonary vascular disease that occurs later in life.

According to the log ratio, we chose to validate on Fgfr2, Notch1 and Rhoc, which are closely related to the development of blood vessels (Online supplemental section 2, http://links.lww.com/HJH/A379). Quantitative RT-PCR showed changes in mRNA expression concordant with the cytosine methylation patterns (Fig. S3a, http://links.lww.com/HJH/A378). Hypermethylations in the promoter regions were found in methylation array profiles of the three genes (*Fgfr2*, *Notch1* and *Rhoc*) in the EUGR samples compared with controls (Fig. S3b, http://links.lww.com/HJH/A378).

DNA methylation and histone modifications patterns of endothelial nitric oxide synthase, peroxisome proliferator-activated receptor gamma and insulin-like growth factor-1 in response to extrauterine growth restriction

To investigate the association between EUGR-induced genes activating epigenetic modification, we analyzed DNA methylation and histone modifications patterns of these three genes in response to EUGR. Total methylation at the eNOS and PPARγ promoter region in EUGR were not different from controls (Fig. 5a, left middle). Methylation at the promoter region was decreased in the EUGR rat PVECs relative to control (Fig. 5a, right, see red box). Hypomethylation at the IGF-1 promoter region in EUGR rats relative to controls may be associated with increased IGF-1 mRNA expression (Fig. 3).

ChIP was used to compare the chromatin state, in terms of a specified set of histone modifications, associated with the DNA sequences of interest regions between EUGR and control (Fig. 5b). These 'activating marks' were H3K4met3 and H3K9ace. The second set of histone modifications were markers classically associated with gene repression (H3K9met3 and H3K27met3). EUGR increased 'repressing 'marks (H3K27met3 and H3K9met3) relative to the control animals in the four sites of eNOS promoter, especially H3K27met3 (Fig. 5b, left). In the five sites along the *PPARγ* gene, both H3K4met3 and H3K9met3 occupancy are higher than that of control (Fig. 5b, middle). Repressive chromatin mark (H3K9met3) plays the dominant role in *PPARγ* gene expression. In the five sites along the *IGF-1* gene, both H3K9ace and H3K27met3 occupancy are higher than that of control (Fig. 5b, right). These results indicate that increased 'repressing marks' (H3K27met3/H3K9met3) are associated with decreased level of eNOS and PPARγ mRNA expression in 9-week-old male rats.

DISCUSSION

Our study showed that EUGR causes pulmonary endothelial dysfunction *in vivo*, which appears to be related to an epigenetic mechanism. One of the epigenetic mechanisms is the regulation of cell-specific and developmental-specific gene expression. Such modulation of gene expression provides a means of fine-tuning during development. In the context of developmental origins, this has been referred to as providing the 'plasticity' needed to optimize the survival during times of perinatal stress. Our study has three major findings. First, EUGR male rats present with pulmonary hypertension during late life. Second, our

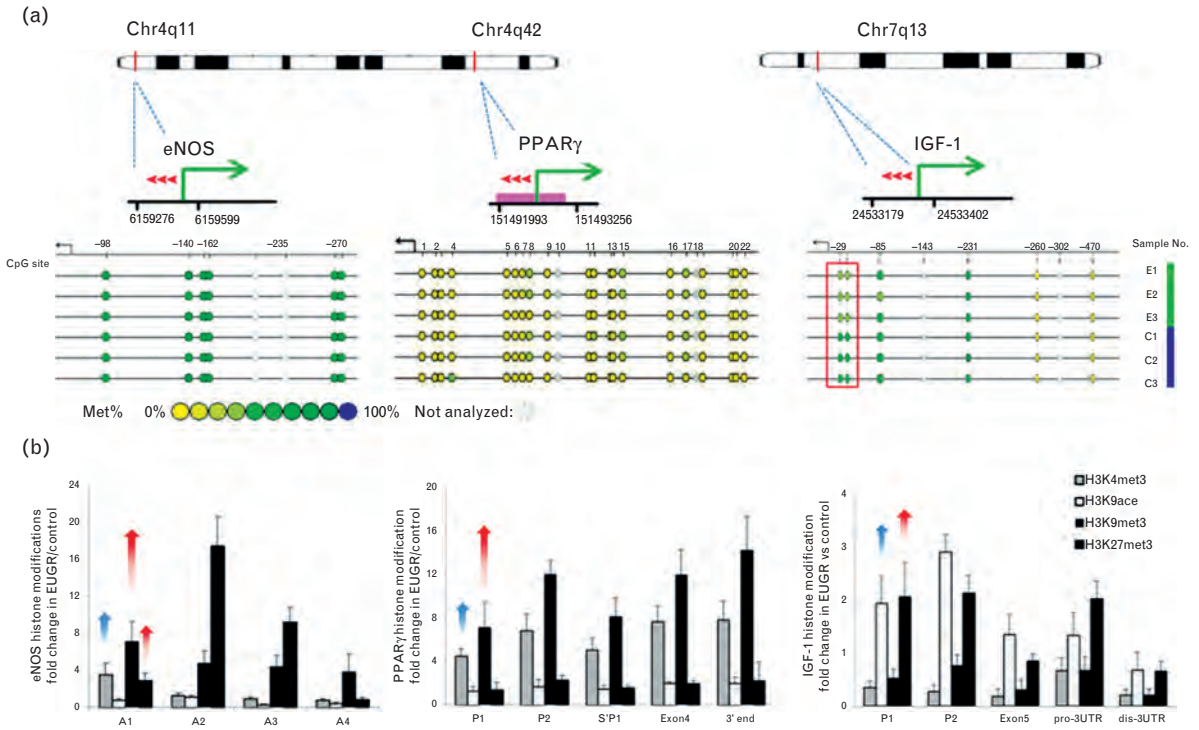

FIGURE 5 DNA methylation status and histone modifications of the *eNOS*, *PPARγ* and *IGF-1* genes in the PVECs of 9-week-old male rats. (a) MassARRAY measurements confirm the DNA methylation status of promoter region in the gene *eNOS* (left), *PPARγ* (middle) and *IGF-1* (right). CpG sites were differently numbered from the proximal promoter area. Red arrowheads represent the relative positions of bisulfite sequenced amplicons. Matlab7.0.4 software was used to assess site-specific CpG methylation. Each line represents a CpG methylation profile of eNOS, PPARγ and IGF-1 promoter region from EUGR ($n = 3$) and control samples ($n = 3$). Colors of each circle represent the methylation level of each corresponding CpG unit. ×, missing data at a given CpG site; met%, percentage of methylation. There was a significant difference between the control and EUGR in the CpG site 1.2. of IGF-1 promoter region (see red box). (b) Histone modifications along the *eNOS* (left), *PPARγ* (middle) and *IGF-1* (right) genes in the PVECs of 9-week-old male rats ($n = 5$–6). Quantitative ChIP analysis of four histone H3 covalent modifications at *eNOS*, *IGF-1* and *PPARγ* genes was shown. Results presented as EUGR fold change of the control ± SEM. The two histone modifications frequently associated with gene activation (H3K4met3 and H3K9ace) are shown by light bars, whereas those commonly associated with gene repression (H3K9met3 and H3K27met3) are shown by dark bars. EUGR increased 'repressing marks' (H3K27met3/H3K9met3) in *eNOS* and *PPARγ* genes, and both H3K9ace and H3K27met3 occupancy are higher than that of the control in *IGF-1* gene. ChIP, chromatin immune precipitation; eNOS, endothelial nitric oxide synthase; EUGR, extrauterine growth restriction; PPARγ, peroxisome proliferator-activated receptor gamma; PVECs, pulmonary vascular endothelial cells.

present study demonstrated that changes in chromatin structure at the *eNOS* gene were associated with its decreased expression in the rat model of EUGR. The differences in histone modifications at the *eNOS* gene between EUGR and controls suggest that epigenetic processes may, at least in part, be responsible for the pathogenesis of pulmonary hypertension. Thirdly, we found that DNA methylation in PVECs was altered in EUGR. We performed a whole-genome cytosine methylation assay on PVECs isolated from 9-week-old male rats. The differences in DNA methylation between EUGR and control groups suggest their putative role on endothelial dysfunction in patients with pulmonary hypertension. These data demonstrate that EUGR affects gene expression, epigenetic characteristics and resets the structure and function of the pulmonary vasculature into adulthood.

Our study reported for the first time that epigenetic dysregulation is a strong candidate for propagating the PVEC memory of early postnatal events, causing changes in the expression of genes and long-term susceptibility to pulmonary hypertension. The endothelium plays a central role in the regulation of vascular tone. Endothelial dysfunction is evident in human low birth weight infants as well as in the experimental models of fetal growth restriction associated with maternal undernutrition during late gestation [8,10,31,32]. A reduction in the bioavailability of nitric oxide is believed to be a major contributor to altered vascular function in the metabolic syndrome and is a key mechanism mediating the age and sex related decline of endothelium-dependent vasodilatation in human adults [33,34]. Recent evidence suggests that the development and progression of vascular disease, including atherosclerosis, coronary heart disease and hypertension, is associated with a reduced nitric oxide production [20]. Increased PVEC levels of eNOS mRNA in PPHN newborn rats has been reported previously. Interestingly, our study found decreased PVEC levels of eNOS and PPARγ mRNA, and increased PVEC levels of IGF-1 mRNA in 9-week-old male rats. These decreased levels of eNOS may cause a reduction of nitric oxide. It suggests that these three genes in PVECs are sensitive to regulation by the EUGR insult.

Changes in gene expression long after the postnatal insult of EUGR can be attributed to epigenetics. The schematic diagram shows the role of epigenetic regulation in vascular endothelial gene expression (Fig. 5b). Epigenetic regulation of gene expression is associated with DNA methylation and changes in multiple histone marks (the interactions between multiple marks) [35,36]. For example, accumulation of H3K4Met3 and H3K9Ace is often thought of as 'activating markers' of gene expression, and

accumulation of H3K9met3/H3K27met3 is often thought of as 'repressing marks' of gene expression [37,38]. Indeed, in our study, increased H3K27met3 and H3K9met3 are associated with decreased PVEC levels of eNOS and PPARγ mRNA expression in 9-week-old male rats. When IGF-1 mRNA levels were significantly increased, methylation of PVECs at the P1 promoter region was decreased in EUGR rats relative to the controls.

In this study, we employed the genome-wide CpG promoter microarrays and MeDIP, a sensitive method, to identify the differentially methylated regions in EUGR vs. control PVEC. We found numerous DMRs, some of which were validated in a cohort of EUGR PVEC by the Sequenom's MassARRAY system. Hence, the MeDIP-chip platform is both efficient and effective. On the other hand, we had to admit that the data had some limitations because our MeDIP-chip study was based on very small number samples. We analyzed the DMRs mapped to the gene promoters in PVEC (Fig. S1, http://links.lww.com/HJH/A378). We found 488 hypomethylated and 216 hypermethylated regions in EUGR. Among them, 244 hypomethylated and 38 hypermethylated regions were mapped to the gene promoters, suggesting that the methylation status may regulate the transcription of these genes. Growing evidence indicates that DNA methylation in the promoter of a gene seems to be in a nonrandom fashion and the methylation patterns vary, depending on the cell types [39]. In addition to the specific methylation patterns, we identified genomic hotspots, which harbor an abundance of the methylated promoter regions. In particular, we found that methylation hotspots contained the promoter-hypermethylated genes predominantly on 1, 5, 12, 14 and 19 chromosomes. A previous study had reported that the methylation hotspots are identified on chromosome 19 in acute lymphoblastic leukemia (ALL) cells [40]. Apparently, the methylation prefers certain regions of genome and these regions are varying in different types of diseases. However, the mechanisms by which various regions of genome are methylated in different types of diseases remain to be further investigated.

We also performed functional and pathway analysis of these differential promoter-methylated genes using the DAVID bioinformatics tools (Fig. S2, http://links.lww.com/HJH/A378) [26]. Functional analysis revealed that these promoter hypermethylated and hypomethylated genes were involved in location, blood circulation, circulatory system process, vascular process in circulatory system, response to stimulus, signaling, response to hormone stimulus and cholesterol metabolic process. Some of the genes, such as events in the calcium, Notch, VEGF, TGF-beta, ErbB, insulin, Wnt and MAPK signal pathways (Fig. S2, http://links.lww.com/HJH/A378), were also involved in regulating the development of pulmonary hypertension. In addition, several of the promoter-hypermethylated genes were associated with the development of pulmonary hypertension and these include Fgfr2 [41], Notch1 [42–44] and Rhoc [45] (Fig. S3, http://links.lww.com/HJH/A378). EUGR changes cytosine methylation at approximately 500 loci in male rats at 9 weeks of age, preceding the development of pulmonary hypertension and these represent the candidate loci for mediating the pathogenesis of pulmonary vascular disease that occurs later in life. Notably, many of them are novel methylation-regulated genes that have not been identified previously in the development of pulmonary hypertension. Moreover, the research strategies and the resulting data are valuable for the evaluation of the significance of DMRs in EUGR PVECs.

Thus, EUGR during infancy is associated with altered PVEC genes expression in association with the specific changes in DNA methylation and histone marks in the PVEC genes in 9-week-old male rats. Several studies have shown the associations between molecular changes in eNOS, IGF-1 and PPARγ with pulmonary hypertension and IUGR [14,15,18]; however, none demonstrated this association in a model of EUGR. We did find these specific molecular changes in PVECs and the degree of the associated pulmonary hypertension in EUGR adult male rats. Some studies showed activation in the renin–angiotensin–aldosterone system (RAAS) is also an important feature associated with metabolic syndrome, and dysregulated RAAS contributes to pulmonary arterial hypertension [46]. However, there are no genes related to RAAS involved in hypermethylation or hypomethylation observed in EUGR rats from our study. The results of our study provide evidence that the adult male rats that underwent EUGR in early infancy exhibit resetting structure and function of the pulmonary vasculature, which increases susceptibility of the PVECs to pulmonary hypertension.

Our study has limitations. Because the rats were too small to separate pulmonary arteries and the amount of tissue needed for the assay, we used the MACS method to purify PVECs from the whole-lung tissues. The isolated PVECs might originate from pulmonary capillaries, arteries and veins, MACS may be an effective method for separating the specific cell types from the tissues [47]. However, it is possible that the *PVEC* gene levels could be different. Although our results suggest that altered PVEC eNOS, IGF-1 and PPARγ expression may play a role in EUGR-associated pulmonary hypertension during adulthood, we will replicate the results of altered gene expression and epigenetic modifications of eNOS, IGF-1 and PPARγ in human endothelial cells *ex vivo* and in cultured human PVECs and assess relevant signaling pathways in the cells *in vitro* in our future study.

In conclusion, our study shows that a postnatal insult, nutritional-restriction-induced EUGR, is associated with altered gene expression and epigenetic characteristics of the PVECs in adult male rats. By using a genome-wide approach, we have uncovered validated changes in cytosine methylation that are associated with local transcriptional dysregulation. In addition, we report novel evidence of pulmonary hypertension in EUGR male rats during adulthood. We speculate that altered eNOS, IGF-1 and PPARγ expression in the EUGR male rat PVECs may play a role in the endothelial dysfunction seen in patients with pulmonary hypertension. Thus, providing adequate nutrients and improving the early postnatal feeding environment and postnatal growth may, particularly in postnatal nutrition of preterm neonates in ICUs, be of benefit in reducing adulthood pulmonary hypertension risk.

ACKNOWLEDGEMENTS

The authors thank Dr Josef Neu from the Division of Neonatology, Department of Pediatrics in the College of Medicine, University of Florida for reviewing this article. The authors also thank Key Laboratory of Reproductive Genetics (Zhejiang University), Ministry of Education and Zhejiang Key Laboratory for Diagnosis and Bioelectromagnetics Laboratory of Zhejiang University School of Medicine for their assistance.

Sources of funding: This work was supported by the grants from the National Natural Science Foundation of China (nos. 81070512, 81270722 and 81200460), National Science and Technology Major Projects for 'Major New Drugs Innovation and Development' (2013ZX09303003), and National Key Technology R&D Program (no. 2012BAI04B04).

Conflicts of interest

There are no conflicts of interest.

REFERENCES

1. Simmons R. Developmental origins of adult metabolic disease. *Endocrinol Metab Clin North Am* 2006; 35:193–204; viii.
2. Nuyt AM. Mechanisms underlying developmental programming of elevated blood pressure and vascular dysfunction: evidence from human studies and experimental animal models. *Clin Sci (Lond)* 2008; 114:1–17.
3. Tare M, Parkington HC, Bubb KJ, Wlodek ME. Uteroplacental insufficiency and lactational environment separately influence arterial stiffness and vascular function in adult male rats. *Hypertension* 2012; 60:378–386.
4. Patel MS, Srinivasan M. Metabolic programming in the immediate postnatal life. *Ann Nutr Metab* 2011; 58 (Suppl. 2):18–28.
5. Wiedmeier JE, Joss-Moore LA, Lane RH, Neu J. Early postnatal nutrition and programming of the preterm neonate. *Nutr Rev* 2011; 69:76–82.
6. Sun C, Burgner DP, Ponsonby AL, Saffery R, Huang RC, Vuillermin PJ, *et al.* Effects of early-life environment and epigenetics on cardiovascular disease risk in children: highlighting the role of twin studies. *Pediatr Res* 2013; 73 (4 Pt 2):523–530.
7. Dakshinamurti S. Pathophysiologic mechanisms of persistent pulmonary hypertension of the newborn. *Pediatr Pulmonol* 2005; 39:492–503.
8. Poston L. Influences of maternal nutritional status on vascular function in the offspring. *Curr Drug Targets* 2007; 8:914–922.
9. Norman M, Martin H. Preterm birth attenuates association between low birth weight and endothelial dysfunction. *Circulation* 2003; 108:996–1001.
10. Touwslager RN, Gerver WJ, Tan FE, Gielen M, Zeegers MP, Zimmermann LJ, *et al.* Influence of growth during infancy on endothelium-dependent vasodilatation at the age of 6 months. *Hypertension* 2012; 60:1294–1300.
11. Moleres A, Campion J, Milagro FI, Marcos A, Campoy C, Garagorri JM, *et al.* Differential DNA methylation patterns between high and low responders to a weight loss intervention in overweight or obese adolescents: the EVASYON study. *FASEB J* 2013; 27:2504–2512.
12. Sebert S, Sharkey D, Budge H, Symonds ME. The early programming of metabolic health: is epigenetic setting the missing link. *Am J Clin Nutr* 2011; 94 (6 Suppl.):1953S–1958S.
13. Canani RB, Costanzo MD, Leone L, Bedogni G, Brambilla P, Cianfarani S, *et al.* Epigenetic mechanisms elicited by nutrition in early life. *Nutr Res Rev* 2011; 24:198–205.
14. Joss-Moore LA, Wang Y, Ogata EM, Sainz AJ, Yu X, Callaway CW, *et al.* IUGR differentially alters MeCP2 expression and H3K9Me3 of the PPARgamma gene in male and female rat lungs during alveolarization. *Birth Defects Res A Clin Mol Teratol* 2011; 91:672–681.
15. Fu Q, Yu X, Callaway CW, Lane RH, McKnight RA. Epigenetics: intrauterine growth retardation (IUGR) modifies the histone code along the rat hepatic *IGF-1* gene. *FASEB J* 2009; 23:2438–2449.
16. Vaiman D, Gascoin-Lachambre G, Boubred F, Mondon F, Feuerstein JM, Ligi I, *et al.* The intensity of IUGR-induced transcriptome deregulations is inversely correlated with the onset of organ function in a rat model. *PLoS One* 2011; 6:1–6; e21222.
17. Rexhaj E, Bloch J, Jayet PY, Rimoldi SF, Dessen P, Mathieu C, *et al.* Fetal programming of pulmonary vascular dysfunction in mice: role of epigenetic mechanisms. *Am J Physiol Heart Circ Physiol* 2011; 301:H247–H252.
18. Xu XF, Ma XL, Shen Z, Wu XL, Cheng F, Du LZ. Epigenetic regulation of the endothelial nitric oxide synthase gene in persistent pulmonary hypertension of the newborn rat. *J Hypertens* 2010; 28:2227–2235.
19. Xu XF, Lv Y, Gu WZ, Tang LL, Wei JK, Zhang LY, Du LZ. Epigenetics of hypoxic pulmonary arterial hypertension following intrauterine growth retardation rat: epigenetics in PAH following IUGR. *Respir Res* 2013; 14:1–20.
20. Franco MC, Higa EM, D'Almeida V, de Sousa FG, Sawaya AL, Fortes ZB, Sesso R. Homocysteine and nitric oxide are related to blood pressure and vascular function in small-for-gestational-age children. *Hypertension* 2007; 50:396–402.
21. Fiorotto ML, Burrin DG, Perez M, Reeds PJ. Intake and use of milk nutrients by rat pups suckled in small, medium, or large litters. *Am J Physiol* 1991; 260:R1104–R1113.
22. Des Robert C, Li N, Caicedo R, Caicedo R, Frost S, Lane R, *et al.* Metabolic effects of different protein intakes after short term undernutrition in artificially reared infant rats. *Early Hum Dev* 2009; 85:41–49.
23. Clark RH, Thomas P, Peabody J. Extrauterine growth restriction remains a serious problem in prematurely born neonates. *Pediatrics* 2003; 111 (5 Pt 1):986–990.
24. Champion HC, Bivalacqua TJ, Greenberg SS, Giles TD, Hyman AL, Kadowitz PJ. Adenoviral gene transfer of endothelial nitric-oxide synthase (eNOS) partially restores normal pulmonary arterial pressure in eNOS-deficient mice. *Proc Natl Acad Sci USA* 2002; 99:13248–13253.
25. Xu XF, Gu WZ, Wu XL, Li RY, Du LZ. Fetal pulmonary vascular remodeling in a rat model induced by hypoxia and indomethacin. *J Matern Fetal Neonatal Med* 2011; 24:172–182.
26. Huang DW, Sherman BT, Lempicki RA. Systematic and integrative analysis of large gene lists using DAVID bioinformatics resources. *Nat Protoc* 2009; 4:44–57.
27. Mar JC, Wells CA, Quackenbush J. Defining an informativeness metric for clustering gene expression data. *Bioinformatics* 2011; 27:1094–1100.
28. Mikkelsen TS, Ku M, Jaffe DB, Issac B, Lieberman E, Giannoukos G, *et al.* Genome-wide maps of chromatin state in pluripotent and lineage-committed cells. *Nature* 2007; 448:553–560.
29. Ehrich M, Nelson MR, Stanssens P, Zabeau M, Liloglou T, Xinarianos G, Cantor CR, *et al.* Quantitative high-throughput analysis of DNA methylation patterns by base-specific cleavage and mass spectrometry. *Proc Natl Acad Sci USA* 2005; 102:15785–15790.
30. Thompson RF, Reimers M, Khulan B, Gissot M, Richmond TA, Chen Q, *et al.* An analytical pipeline for genomic representations used for cytosine methylation studies. *Bioinformatics* 2008; 24:1161–1167.
31. Martin H, Hu J, Gennser G, Norman M. Impaired endothelial function and increased carotid stiffness in 9-year-old children with low birthweight. *Circulation* 2000; 102:2739–2744.
32. Payne JA, Alexander BT, Khalil RA. Reduced endothelial vascular relaxation in growth-restricted offspring of pregnant rats with reduced uterine perfusion. *Hypertension* 2003; 42:768–774.
33. Donato AJ, Eskurza I, Silver AE, Levy AS, Pierce GL, Gates PE, Seals DR. Direct evidence of endothelial oxidative stress with aging in humans: relation to impaired endothelium-dependent dilation and upregulation of nuclear factor-kappaB. *Circ Res* 2007; 100:1659–1666.
34. Gao L, Mann GE. Vascular NAD(P)H oxidase activation in diabetes: a double-edged sword in redox signalling. *Cardiovasc Res* 2009; 82:9–20.
35. Bruce KD, Hanson MA. The developmental origins, mechanisms, and implications of metabolic syndrome. *J Nutr* 2010; 140:648–652.
36. Matouk CC, Marsden PA. Epigenetic regulation of vascular endothelial gene expression. *Circ Res* 2008; 102:873–887.
37. Bloom DC, Giordani NV, Kwiatkowski DL. Epigenetic regulation of latent HSV-1 gene expression. *Biochim Biophys Acta* 2010; 1799:246–256.
38. Taverna SD, Ilin S, Rogers RS, Tanny JC, Lavender H, Li H, *et al.* Yng1 PHD finger binding to H3 trimethylated at K4 promotes NuA3 HAT

activity at K14 of H3 and transcription at a subset of targeted ORFs. *Mol Cell* 2006; 24:785–796.
39. Weber M, Davies JJ, Wittig D, Oakeley EJ, Haase M, Lam WL, Schubeler D. Chromosome-wide and promoter-specific analyses identify sites of differential DNA methylation in normal and transformed human cells. *Nat Genet* 2005; 37:853–862.
40. Taylor KH, Pena-Hernandez KE, Davis JW, Arthur GL, Duff DJ, Shi H, *et al*. Large-scale CpG methylation analysis identifies novel candidate genes and reveals methylation hotspots in acute lymphoblastic leukemia. *Cancer Res* 2007; 67:2617–2625.
41. Friedmacher F, Doi T, Gosemann JH, Fujiwara N, Kutasy B, Puri P. Upregulation of fibroblast growth factor receptor 2 and 3 in the late stages of fetal lung development in the nitrofen rat model. *Pediatr Surg Int* 2012; 28:195–199.
42. Taichman DB, Loomes KM, Schachtner SK, Guttentag S, Vu C, Williams P, *et al*. Notch1 and Jagged1 expression by the developing pulmonary vasculature. *Dev Dyn* 2002; 225:166–175.
43. Boucher JM, Peterson SM, Urs S, Zhang C, Liaw L. The miR-143/145 cluster is a novel transcriptional target of Jagged-1/Notch signaling in vascular smooth muscle cells. *J Biol Chem* 2011; 286:28312–28321.
44. Takeshita K, Satoh M, Ii M, Silver M, Limbourg FP, Mukai Y, *et al*. Critical role of endothelial Notch1 signaling in postnatal angiogenesis. *Circ Res* 2007; 100:70–78.
45. Wang W, Wu F, Fang F, Tao Y, Yang L. RhoC is essential for angiogenesis induced by hepatocellular carcinoma cells via regulation of carcinoma cells via regulation of endothelial cell organization. *Cancer Sci* 2008; 99:2012–2018.
46. De Man FS, Tu L, Handoko ML, Rain S, Ruiter G, Francois C, *et al*. Dysregulated renin–angiotensin–aldosterone system contributes to pulmonary arterial hypertension. *Am J Respir Crit Care Med* 2012; 186:780–789.
47. Sobczak M, Dargatz J, Chrzanowska-Wodnicka M. Isolation and culture of pulmonary endothelial cells from neonatal mice. J Vis Exp 2010; 46:e2316, 1–4.

Reviewers' Summary Evaluations

Referee 1

Zhang and coworkers evaluated the epigenetic (DNA methylation and histone marks) of postnatal induced growth restriction on the lungs of 9-week rats. They discovered differences in DNA methylation at 500 loci near genes involved in c-AMP and cholesterol metabolic processes, cell growth, transport, and present an epigenetic landscape of the maturing lung in a stressful environment. Genes predicted to be involved in this context (eNOS, PPARγ and IGF1) were studied as well, and epigenetic differences linked with their expression were revealed. Although results in rodents do not predict what can be found in humans, where lung maturation presents with a different kinetics, this original study improves our understanding of epigenetic consequences of stress on sensitive developing organs.

Referee 2

The purpose of the study was to assess whether epigenetics dysregulation may be involved in the effects of nutritional disadvantages during early postnatal life on pulmonary vascular consequences in later life, since a postnatal insult, such as extrauterine growth restriction (EUGR), may cause epigenetic modification of the genes related to lung development and pulmonary vascular tone regulation in later life. To test this hypothesis, the Authors developed a EUGR rat model by postnatal nutritional restrictions. The Authors concluded that epigenetics dysregulation is a strong mechanism for propagating the cellular memory of early postnatal events, causing changes in expression of genes and long term susceptibility to pulmonary hypertension. The manuscript is well written and the topic interesting.